

Search for stimulated photon-photon scattering in vacuum

D. Bernard^{1,a}, F. Moulin², F. Amiranoff³, A. Braun⁴, J.P. Chambaret⁴, G. Darpentigny⁴, G. Grillon⁴, S. Ranc⁴, and F. Perrone⁵

¹ Laboratoire de Physique Nucléaire et des Hautes Énergies, École Polytechnique, IN2P3 & CNRS, 91128 Palaiseau, France

² Laboratoire de Physique, École Normale Supérieure, 94235 Cachan, France

³ Laboratoire pour l'Utilisation des Lasers Intenses^b, École Polytechnique, 91128 Palaiseau, France

⁴ Laboratoire d'Optique Appliquée, CNRS & ENSTA, École Polytechnique, 91128 Palaiseau, France

⁵ Dipartimento di Fisica-Pisa and INFN, Piazza Torricelli 2, 56100 Pisa, Italy

Received 29 September 1999

Abstract. We have searched for stimulated photon scattering in vacuum at a center of mass photon energy of 0.8 eV. The QED contribution to this process is equivalent to four wave mixing in vacuum. No evidence for $\gamma\gamma$ scattering was observed. The corresponding upper limit of the cross-section is $\sigma_{\text{Lim}} = 1.5 \times 10^{-48} \text{ cm}^2$.

PACS. 13.85.Dz Elastic scattering – 12.20.Fv Experimental tests – 78.45.+h Stimulated emission

1 Introduction

Photon-photon scattering does not occur in classical electrodynamics because Maxwell's equations are linear in the fields. In Quantum ElectroDynamics (QED), $\gamma\gamma$ elastic scattering is described in lowest order by a fermion loop with four open photon lines (box diagram). At low energies ($\hbar\omega \ll mc^2$), the corresponding cross-section is $\sigma_{\text{QED}} = (973/10125\pi)\alpha^2 r_e^2 (\hbar\omega/mc^2)^6$ where $\hbar\omega$ is the center of mass system (cms) photon energy, m is the electron mass, α is the fine structure constant, and r_e is the classical radius of the electron [1]. This cross-section is extremely small in the optical domain where high brightness sources exist: $\sigma_{\text{QED}}[\text{cm}^2] = 7.3 \times 10^{-66} (\hbar\omega[\text{eV}])^6$.

QED is a well established theory. The derivation of σ_{QED} is not in question. Furthermore, the contribution of the box diagram is needed to describe the already observed Delbrück scattering and the high precision measurements of the electron and muon magnetic moment.

The interest here is in the search for possible non-QED new physics in low energy $\gamma\gamma$ scattering. A theoretical basis for this is possibly coming from composite photon theory [2] or the exchange of an axion [3].

A previous experiment using the head-on collision of two laser beams at different wavelengths has obtained a limit cross-section of 10^{-39} cm^2 (at 95% CL) [4]. Here we improve this result by nine orders of magnitude by stimulating the reaction with a third beam [5–8]. The QED contribution to this process is equivalent to four wave mixing in vacuum.

2 The choice of the configuration

In elastic scattering, the values of the energies e_i and wave vectors \mathbf{k}_i of the incoming photons satisfy the energy-momentum conservation condition: $e_1 + e_2 = e_3 + e_4$, $\mathbf{k}_1 + \mathbf{k}_2 = \mathbf{k}_3 + \mathbf{k}_4$, where indices 1, 2 denote the incoming photons, 3, 4 the outgoing photons.

In simple (*i.e.* non stimulated) elastic scattering, the final state is determined by two parameters (*e.g.* the Euler angles of the decay axis in the cms). Here we stimulate the reaction by a third beam, with a wavelength λ_3 ; this fixes one parameter. The direction of beam #3 must lie on the cone of allowed direction for a scattered photon at λ_3 . This position on the cone then fixes the second parameter. The signal is then searched for in the direction of $\mathbf{k}_4 = \mathbf{k}_1 + \mathbf{k}_2 - \mathbf{k}_3$. We have chosen to use three IR beams ($\lambda_1 = \lambda_2 = 800 \text{ nm}$, $\lambda_3 = 1300 \text{ nm}$), with the signal expected in the visible ($\lambda_4 = (2/\lambda_1 - 1/\lambda_3)^{-1} = 577 \text{ nm}$).

In this configuration, the photons of the input beams that scatter in the residual plasma or on the optics can be spatially and spectrally filtered out, and the signal can be easily detected. For strong signal isolation, the wavelength of the signal is also chosen to be far from the wavelengths of the harmonics of the input beams, which are always present in a high intensity beam.

The 3 beams are focused by a single optics made of a pair of spherical mirrors (Bowen) with a coronal pupil of width 30 mm, and an equivalent focal length of 100 mm. The paraxial surface of the Bowen is a cone with a half angle of 33.6° . A left-right symmetric configuration is chosen (Fig. 1) with the main beams at an angle φ with respect to the vertical direction; with $\cos(\varphi) = 1 - \lambda_1/\lambda_3$, we have $\varphi = 67.4^\circ$. As the three beams are injected on that cone, the expected signal lies also on the cone.

^a e-mail: denis.bernard@in2p3.fr

^b Unité mixte N° 7605 du CNRS-CEA-École Polytechnique-Université Paris 6.

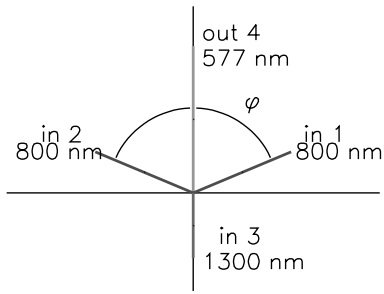


Fig. 1. Angular configuration of the stimulated experiment. The projection of the wave vectors \mathbf{k}_i of the four beams on the pupil plane of the Bowen are shown.

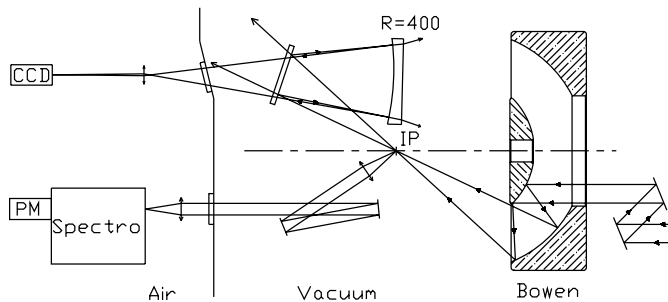


Fig. 2. Layout of the experimental apparatus. Only beam #3 is shown.

The characteristics of the beams are chosen so as to optimize their overlap at the interaction point (IP). The optimum is obtained for beams with the waist w on the order of the FWHM bunch length $c\tau$.

3 Experimental apparatus

The two main beams (#1 and #2) at 805 nm are produced by a Ti: sapphire chirped pulse amplification (CPA) laser chain with 3 amplifying stages [9]. Gaussian beams with 0.4 J of energy, 55 nm spectral width, and 40 fs FWHM duration are delivered at 10 Hz. A pair of tunable frustrated internal reflection attenuators allows the reduction of the intensity of the main beams without degrading their optical quality or modifying their angle and temporal synchronization. Then, the two beams enter a vacuum chamber where they are expanded to a diameter $\phi = 30$ mm. The chirped pulses are temporally compressed to 40 fs, and are transported to the experimental chamber.

A fraction of the beam is collected after the second amplification stage to pump the optical parametric amplifier (OPA) that produces the beam at 1300 nm.

The 3 beams are injected into the Bowen with a diameter ϕ of 30 mm. A low intensity image of the focal spot of each beam is obtained outside the chamber with a unit magnification by a combination of a silica slide and of a non coated silica spherical mirror (Fig. 2). The image is enlarged by a microscope objective with a magnification of 40 (20 for the 1300 nm beam for which the CCD sensitivity is low) onto a CCD camera.

A set of dielectric mirrors with graded reflectivities at 800 nm are used as filters down to an optical density of $D = 3$, before and after the objective. Typical spot sizes at $1/e^2$ in intensity, w , of $4 \mu\text{m}$ (main beams) and $6 \mu\text{m}$ (1300 nm beam) are obtained.

The expected signal photons are collected by a telescope with an f number of 1.9, imaged onto the entrance slit of a spectrometer with a transmission factor of 59% at 577 nm, and detected with a photomultiplier (PMT) with an efficiency of 5%. A BG38 filter further blocks the IR photons. The signal from the PMT is 10 ns in duration at the foot and is digitized by a CAMAC ADC with a gate of 25 ns.

4 Experimental procedure

The relative alignment and synchronization procedures of the three beams at the IP are dependent on each other due to the configuration used. They are performed in several steps. First, the three beams are prealigned at IP on a single camera located on the axis of the Bowen, using a microscope objective with a large numerical aperture of 0.65, and their waists are brought into a common plane perpendicular to that axis. The position of the 3 spots in that plane is adjusted so as to minimize their aberrations. Then, a pre-synchronization of the laser pulses is performed with a precision of 25 ps with a fast diode and a 7 GHz oscilloscope. The fine alignment is obtained by having each laser punch the same hole in a $10 \mu\text{m}$ thick aluminum foil. The synchronization is then refined down to 100 fs by observing the perturbation of the focal spot of a low energy beam after a plasma was created by a high energy beam in a nitrogen gas jet with a pressure of about 0.3 bar. At last, the fine synchronization is performed by observing four wave mixing ($\chi^{(3)}$) in the gas jet.

For this last step, the laser intensities are tuned just below plasma threshold. This method results in the spatial alignment and the synchronization of the beams with the upmost precision. Furthermore it maximizes the signal in exactly the same configuration as that for the experiment in vacuum. This point is detailed in the following section.

5 Four wave mixing and QED stimulated photon scattering

Four wave mixing is a non linear process that appears in the interaction of high intensity light beams in a medium. The evolution of the fields in the medium are described by Maxwell's equation in a non magnetic medium:

$$\nabla^2 \mathcal{E} - \frac{1}{c^2} \frac{\partial^2 \mathcal{E}}{\partial t^2} = \frac{4\pi}{c^2} \frac{\partial^2 \mathcal{P}}{\partial t^2} \quad (1)$$

where the polarization of the medium is developed as a function of the field in the "constitutive" relations:

$$\mathcal{P}(t) = \underline{\chi}^{(1)} \mathcal{E}(t) + \underline{\chi}^{(2)} \mathcal{E}^2(t) + \underline{\chi}^{(3)} \mathcal{E}^3(t) + \dots \quad (2)$$

Here we study the interaction of three incoming beams. We see that a source term is present, that is proportional to $\mathcal{E}^3(t)$. In particular, it contains a term proportional to $e^{i(\omega_4 t - \mathbf{k}_4 \cdot \mathbf{r})}$ with¹ $\mathbf{k}_4 = \mathbf{k}_1 + \mathbf{k}_2 - \mathbf{k}_3$ and $\omega_4 = k_4 c$. A paraxial formulation for that component \mathcal{E}_4 along \mathbf{k}_4 , in the slow varying wave approximation gives:

$$\frac{d\mathcal{E}_{04}}{dz} = -\frac{i\omega_4}{2c}\chi^{(3)}\mathcal{E}_{01}\mathcal{E}_{02}\mathcal{E}_{03} \quad \text{with} \quad \frac{d}{dz} = \frac{\partial}{\partial z} + \frac{1}{c}\frac{\partial}{\partial t}. \quad (3)$$

Let's now turn to QED stimulated photon scattering in vacuum. The insertion of the Euler-Heisenberg correction term [10] in Maxwell's equations gives:

$$\nabla^2 \mathcal{E} - \frac{1}{c^2} \frac{\partial^2 \mathcal{E}}{\partial t^2} = \mu_0 \left[\frac{\partial}{\partial t} \nabla \wedge \mathcal{M} + \frac{\partial^2 \mathcal{P}}{\partial t^2} - c^2 \nabla (\nabla \cdot \mathcal{P}) \right], \quad (4)$$

with

$$\mathcal{P} = 2a [2(\mathcal{E}^2 - c^2 \mathcal{B}^2)\mathcal{E} + 7c^2(\mathcal{E} \cdot \mathcal{B})\mathcal{B}],$$

$$\mathcal{M} = 2a [-2c^2(\mathcal{E}^2 - c^2 \mathcal{B}^2)\mathcal{B} + 7c^2(\mathcal{E} \cdot \mathcal{B})\mathcal{E}],$$

and $a = \hbar e^4 / (360\pi^2 m^4 c^7)$. Under the same approximations as for 4 wave mixing in a medium, we get:

$$\frac{d\mathcal{E}_{04}}{dz} \mathbf{u}_4 = -\frac{i\mu_0 \omega_4}{2} [(c\mathcal{P}_{0x} + \mathcal{M}_{0y})\mathbf{u}_x + (c\mathcal{P}_{0y} - \mathcal{M}_{0x})\mathbf{u}_y] \quad (5)$$

$$\rightarrow \frac{d\mathcal{E}_{04}}{dz} = -\frac{i\omega_4}{2c} \frac{2\hbar e^4 K}{360\pi^2 m^4 c^7 \epsilon_0} \mathcal{E}_{01}\mathcal{E}_{02}\mathcal{E}_{03} \quad (6)$$

K is a factor that depends on the directions of the incident beams and of their polarization ($K < 14$). In our configuration, we have $K \approx 0.56$ [11].

The equations describing the growth rate of \mathcal{E}_{04} of 4 wave mixing in a low pressure gas (Eq. (3)) and of stimulated photon scattering in vacuum (Eq. (6)) have the same form. Therefore we can define [11] the QED susceptibility of vacuum:

$$\begin{aligned} \chi_v^{(3)} &= \frac{2\hbar e^4 K}{360\pi^2 m^4 c^7 \epsilon_0} = \frac{K}{45\pi\alpha} \left(\frac{r_e e}{mc^2} \right)^2 \\ &\approx 3.0 \times 10^{-41} K \text{ (m}^2/\text{V}^2\text{)}. \end{aligned} \quad (7)$$

6 Experimental results

6.1 Four wave mixing in a gas

The typical sensitivity of the delay of the third beam is on the order of 20 fs, which shows that the duration of the

¹ In vacuum the four beams have the same phase velocity, so that the equation $\Delta \mathbf{k} = \mathbf{k}_1 + \mathbf{k}_2 - \mathbf{k}_3 - \mathbf{k}_4 = \mathbf{0}$ holds exactly. In a low pressure gas, the refractive indices at the four wavelengths are close enough so that $\Delta \mathbf{k} \approx 0$, *i.e.* more precisely $w\Delta k \ll 1$.

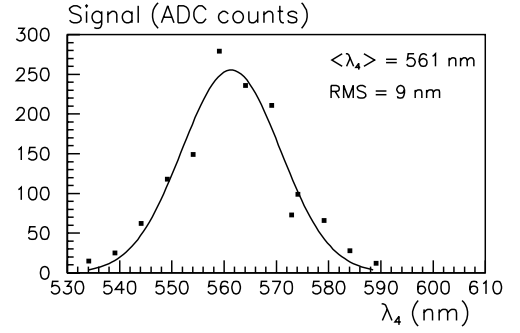


Fig. 3. Spectrum of the $\chi^{(3)}$ signal, with a Gaussian fit. The maximal value in 200 shots is shown as a function of the central value of the spectrometer, with an exit slit of 3 mm, equivalent to a spectral range of 9 nm.

beam provided by the OPA is similar to that of the pump beam.

The main source of fluctuation of the $\chi^{(3)}$ signal is caused by a vertical oscillation of beam #2 due to the pumping system of the compressor. This produces a periodic variation of the signal with an average loss factor equal to 5. The search of a signal in vacuum was interspersed by the observation of the $\chi^{(3)}$ signal in the gas jet. This signal showed an excellent long term stability: after a fraction of an hour the $\chi^{(3)}$ signal was still present, and of the same order of magnitude. The $\chi^{(3)}$ signal was observed with laser energies set just below plasma threshold. We can obtain an upper bound of this laser energy from the intensity threshold I_1 of ionization of nitrogen, close to 10^{14} W/cm²:

$$E = \frac{\pi^{3/2}}{4\sqrt{\ln 2}} \tau I_1 w^2 \quad (8)$$

that is $E \approx 1 \mu\text{J}$. Up to 5×10^4 photons were observed.

The origin of the signal is identified as four wave mixing in the gas, because it is present only with the three beams injected. Furthermore, its spectrum is found to peak at the wavelength λ_4 of four wave mixing (Fig. 3).

The FWHM spectral width, $\Delta\lambda_4 = 22$ nm, corresponds to a Fourier limited FWHM duration of 22 fs. To our knowledge, this is the first observation of large angle four wave mixing.

We compute the expected number of observed scattered photons from the integration of equation (3). We get approximately:

$$N_{4,N_2} = \epsilon_{\text{PM}} \epsilon_{\text{Sp}} \epsilon_{\text{Osc}} \frac{128}{\pi\sqrt{3}} \frac{(\hbar\omega_4)E_1 E_2 E_3}{e^4 w^2 (c\tau)^2} (\chi_{N_2}^{(3)})^2 \quad (9)$$

where E_i are the energy of the three incoming laser pulses, ϵ_{PM} , ϵ_{Sp} , ϵ_{Osc} , are the quantum efficiency of the PMT, the transmission of the spectrometer, and the loss factor due to a transverse oscillation of beam 2.

The third order susceptibility of nitrogen has been measured by other experiments, in different configurations. Nibbering *et al.* have measured the red shift of short pulse spectra due to self phase modulation (SPM) [13]. The value of the nonlinear refractive index, measured

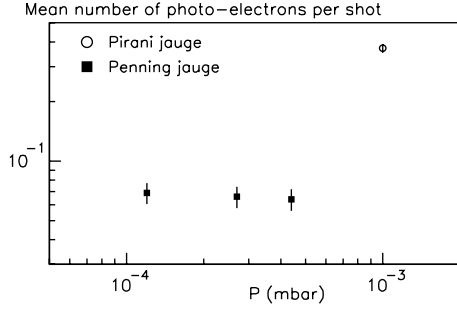


Fig. 4. Pressure dependence of the noise.

at 1 bar, is $n_2 = 2.3 \times 10^{-23} \text{ m}^2/\text{W}$ [13]. That value of n_2 is related to the third order susceptibility by: $n_2 = \chi_{\text{N}_2, \text{SPM}}^{(3)}/(c\epsilon_0)$, so that $\chi_{\text{N}_2, \text{SPM}}^{(3)} \approx 6.1 \times 10^{-26} \text{ m}^2/\text{V}^2$.

Note that the ratio of the third order susceptibilities in vacuum and in gas with pressure P_{bar} is $\chi_v^{(3)}/\chi_{\text{N}_2, \text{SPM}}^{(3)} \approx 4.8 \times 10^{-16} K/P_{\text{bar}}$: the QED vacuum is indeed linear to a very good approximation. The two contributions (four wave mixing in a gas and QED stimulated photon scattering) are of the same order of magnitude only for a pressure close to $P_{\text{Lim}} \approx 4.8 \times 10^{-13} K \text{ mbar}$.

Here, at a pressure of about 0.3 bar, the expected number of photons is $N_{4, \text{N}_2} = 3.5 \times 10^6$.

The value of $\chi_{\text{N}_2}^{(3)}$ has been also measured by Lehmeier *et al.* in third harmonic generation (THG) in nitrogen by a picosecond Nd:glass laser pulse [14]. The obtained value, $\chi_{\text{N}_2, \text{THG}}^{(3)} = 6.7 \times 10^{-27} \text{ m}^2/\text{V}^2$, is about ten times lower than for self phase modulation, and the corresponding value of N_{4, N_2} is 4.2×10^4 .

These numbers are of the same order of magnitude of the number of photons observed in this experiment.

6.2 Stimulated photon scattering in vacuum

A signal was searched for in vacuum with laser energies of 150 mJ, 55 mJ and 200 μJ , and with a spectral acceptance of 30 nm. After compression, transport, and taking into account only the energy that is contained in the central spot at focus, only a fraction of the laser energy is actually available. An estimate of that fraction has been obtained by a subsequent experiment, that has studied precisely the threshold of helium ionization by a single beam [15]. We use here a conservative number of 3%.

At high residual pressure ($P > 5 \times 10^{-4} \text{ mbar}$), we observe a BG noise from the residual plasma (Fig. 4). The one photo-electron signal is easily identified from the pedestal (Fig. 5).

At lower pressure, the remaining noise is due to the creation of white light on a specific imperfect part of the optics that could not be fixed.

Data were taken at 10^{-4} mbar , with an integration time of 100 s; that is 1000 laser shots. For most of the laser shots, no photo-electron (γ_{e^-}) was detected in the

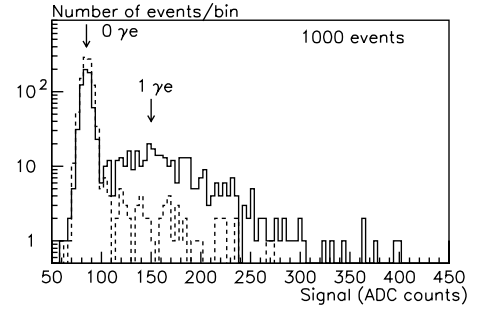


Fig. 5. Spectrum of the signal for pressure $P = 10^{-3} \text{ mbar}$ (solid line), and $P = 1.7 \times 10^{-4} \text{ mbar}$ (dashed line). The signal from the PMT was amplified with gain 80 before digitization. The one photo-electron spectrum is clearly visible over the pedestal (no photo-electron).

PMT. The number of laser shots, with at least $1\gamma_{e^-}$ is presented in the following table.

beam 1 alone	$19\gamma_{e^-}$
beam 2 alone	$42\gamma_{e^-}$
beam 3 alone	$5\gamma_{e^-}$
total	$66\gamma_{e^-}$

3 beams together $60\gamma_{e^-}$

No evidence for an excess non linear contribution of the three beams was observed.

7 Experimental limit of the elastic cross-section

We derive an upper bound of the elastic cross-section by the use of a given model – “chosen to be” here QED:

$$\sigma_{\text{Lim}} = \frac{N_{4, \text{obs}}}{N_{4, \text{QED}}} \sigma_{\text{QED}}. \quad (10)$$

We compute the expected number of scattered photons $N_{4, \text{QED}}$ from the integration of equation (6). We get approximately:

$$N_{4, \text{QED}} = \epsilon_{\text{PM}} \epsilon_{\text{Sp}} \epsilon_{\text{Osc}} \frac{16}{2025} \left(\frac{2}{\pi\sqrt{3}} \right)^3 \times \frac{(\hbar\omega_4) E_1 E_2 E_3}{(mc^2)^4} \frac{r_e^4}{w^2 (c\tau)^2} K^2 \quad (11)$$

where E_i are the energy of the three incoming laser pulses, ϵ_{PM} , ϵ_{Sp} , ϵ_{Osc} , are the quantum efficiency of the PMT, the transmission of the spectrometer, and the loss factor due to a transverse oscillation of beam 2.

We obtain finally a QED prediction of $N_{4, \text{QED}} \approx 7 \times 10^{-21}$ per shot while the observed limit is $N_{4, \text{obs}} \approx 6 \times 10^{-3}$ per shot. The elastic QED cross-section at $\hbar\omega = 0.8 \text{ eV}$ is $\sigma_{\text{QED}} = 1.8 \times 10^{-66} \text{ cm}^2$. The obtained limit is therefore $\sigma_{\text{Lim}} = 1.5 \times 10^{-48} \text{ cm}^2$, that is 18 orders of magnitude from QED (Fig. 6).

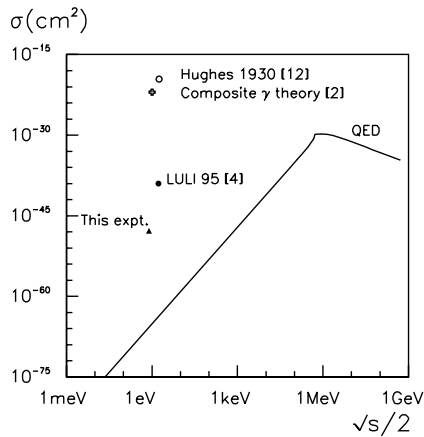


Fig. 6. Elastic photon cross-section as a function of photon cms energy.

8 Conclusion

We have searched for stimulated photon scattering at a cms photon energy of 0.8 eV. The spatial and temporal overlap of three $4 \mu\text{m}$, 40 fs laser beams has been obtained. The last step in the alignment procedure is the maximisation of four wave mixing in a gas in exactly the same configuration as for $\gamma\gamma$ scattering. To our knowledge, this is the first observation of large angle 4 wave mixing in a gas.

In vacuum, no evidence for $\gamma\gamma$ scattering was observed. We obtain an approximate improved upper limit of the cross-section of $\sigma_{\text{Lim}} = 1.5 \times 10^{-48} \text{ cm}^2$, at 18 orders of magnitude from QED. This is an improvement of nine orders of magnitude compared to the previous, non stimulated experiment[4].

Several orders of magnitude could be gained by an improvement in the operation of the laser, the OPA, by an increase of the available fraction of the laser energy in the central spot at focus, by further work on the background noise, and by fixing the transverse oscillation of one beam.

The actual observation of the QED effect will wait for the availability of short pulse lasers in the 10 J class, probably in the next decade.

This work has been funded by Training and Mobility of Researchers contracts # ERBFMGECT950019.

References

1. B. De Tollis, *Nuovo Cimento* **35**, 1182 (1965); B. De Tollis, *Nuovo Cimento* **32**, 757 (1964).
2. P. Raychaudhuri, *Phys. Essays* **2**, 339 (1989); P. Bandyopadhyay, P. Raychaudhuri, *Phys. Rev. D* **3**, 1378 (1971); D. Eimerl, *J. Quant. Spectrosc. Radiat. Transfer* **19**, 473 (1978); D. Eimerl, *J. Quant. Spectrosc. Radiat. Transfer* **25**, 573 (1981).
3. D. Bernard, *Nuovo Cimento A* **110**, 1339 (1997).
4. F. Moulin, D. Bernard, F. Amiranoff, *Z. Phys. C* **72**, 607 (1996).
5. N. Kroll, *Phys. Rev.* **127**, 1207 (1962); see footnote #9.
6. A.A. Varfolomeev, *Sov. Phys. JETP* **23**, 681 (1966).
7. R.L. Dewar, *Phys. Rev. A* **10**, 2107 (1974).
8. G. Grynberg, J.Y. Courtois, *C.R. Acad. Sci. Paris* **311**, 1149 (1990).
9. A. Antonetti *et al.*, *Appl. Phys. B* **65**, 197 (1997).
10. H. Euler, *Ann. Physik* **36**, 398 (1936).
11. F. Moulin, D. Bernard, *Opt. Commun.* **164**, 137 (1999).
12. A.L. Hughes, G.E. Jauncey, *Phys. Rev.* **36**, 773 (1930).
13. E.T.J. Nibbering *et al.*, *J. Opt. Soc. Am. B* **14**, 650 (1997).
14. H.J. Lehmeier *et al.*, *Opt. Commun.* **56**, 67 (1985).
15. J.R. Marquès (private communication).